Sedimentation and Water Electrolysis Effects in Electrofiltration of Kaolin Suspension

O. Larue and E. Vorobiev
Chemical Engineering Dept., University of Compiègne, Compiègne, BP 20529-60205, France

DOI 10.1002/aic.10227
Published online in Wiley InterScience (www.interscience.wiley.com).

Filtration combined with an electric field (electrofiltration) enhances the filtration kinetics of aqueous suspensions. Although electrophoresis and electroosmosis largely contribute to electrofiltration behavior, side effects such as water electrolysis, heat production, and gravitational sedimentation of particles may be influential. A mathematical model was developed to include gravitational sedimentation of particles and electrolytic gas in electrofiltration theory. The model successfully represented electrofiltration data obtained from kaolin suspensions with a laboratory horizontal filter. Electrolytic gas contributed to an increase of 13% in electrofiltration rate. Settling particles increased cake resistance to downward electrofiltration flow and could substantially offset electrokinetic effects at high settling velocities. Because of electrolysis ionic products, a decrease of pH occurred in the filter during electrofiltration, causing the coagulation of kaolin particles and an increase in hydraulic cake permeability. Subsequent filtration could then take place rapidly without any electric field. The overall processing time was decreased by half when an electric field is applied only for 37% of the processing time. This coagulation phenomenon seems to be a promising means to accelerate the filtration kinetics without the need for full-time electrofiltration. © 2004 American Institute of Chemical Engineers *AIChE J,* 50: 3120–3133, 2004

Introduction

Inherent properties of fine particles dispersed in aqueous suspensions are at the origin of extended cake formation times. A combination of mechanical and electrical filtration (that is, electrofiltration) can be effective in enhancing filtrate removal. In a DC electric field, a significant acceleration of filtration rate was observed for various mineral suspensions such as gelatinous bentonite (Moulik, 1971), kaolin (Vorobiev and Jany, 1999), quartz sand (Weber and Stahl, 2002), calcium carbonate (Yukawa et al., 1976), and for biological materials (Iritani et al., 1992). Previous authors showed that the filtration rate becomes more pronounced with increasing field strength and the electrokinetic potential of particles. Particles in aqueous solutions acquire a surface charge creating an electrokinetic potential, caused by ion dissociation, ion absorption, or ion dissolution. An electric field applied between two electrodes can then move suspended particles relative to the liquid (electrophoresis) or move the liquid relative to a fixed layer of charged particles (electroosmosis). In electrofiltration, both phenomena take place. In an electric field of proper polarity, electrophoresis reduces the rate of cake formation and increases the rate of permeation through the filter cake by electroosmosis.

A DC electric field can also increase the efficiency of other operations performed on industrial filters. Numerous publications show that combining a DC electric field with mechanical compression of filter cakes is very effective (pressurized electroosmotic dewatering or deliquoring; Barton et al., 1999; Iwata et al., 1991; Orsat et al., 1999). Recently, the application of DC electric fields during the washing operation (electrowashing) was studied. The very interesting effect of selective removal of charged species during electrowashing was demonstrated (Tarleton et al., 2003). Electrically assisted filtration

Correspondence concerning this article should be addressed to O. Larue at olivier.larue@utc.fr

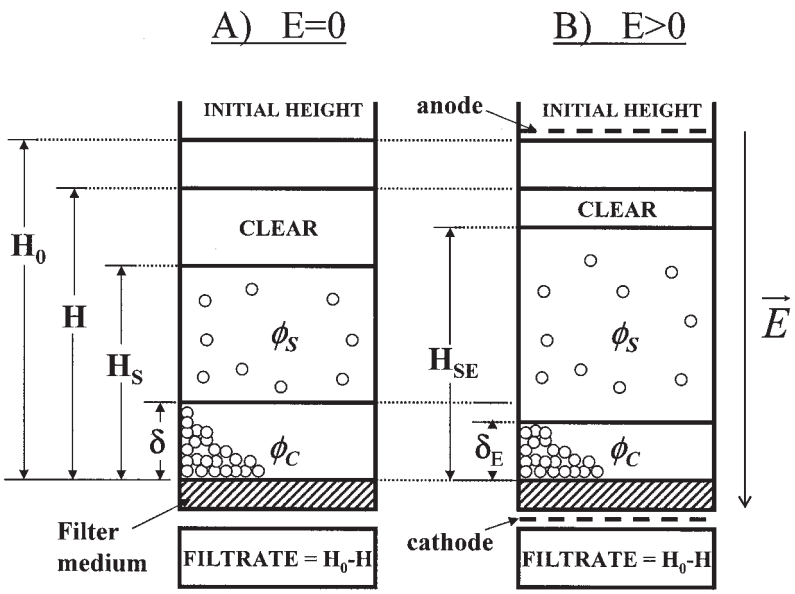

Figure 1. Quantities involved in filtration with sedimentation (A) and electrofiltration with sedimentation (B).

and compression of filter cakes are now advanced at the pilot scale and have revealed promising results. Electrical devices are easily adaptable to the technology of industrial filters such as plate filter press (Kondo and Hiraoka, 1990) and belt filter press (Raats et al., 2002).

Difficulties still subsist in the industrialization of the electrofiltration process. A continuous electric field is rather criticized for its high-energy requirements, and current flow side effects such as heat production and reactions at the electrodes. Even though these side effects might significantly improve the electrofiltration process, only few authors are concerned with them. The electrolytic gases (O_2 and H_2) generated during water electrolysis at the electrodes can accelerate electrofiltration and slightly improve the residual moisture of the final filter cake (Weber and Stahl, 2002). Water electrolysis also generates the ionic species H_3O^+ and OH^- that may destabilize the colloidal suspension, leading to transient coagulation of particles. It is worth mentioning that just as in electrowashing, displacement of ionic species in the electric field is important in the electrofiltration process. Because of the production of H_3O^+ at the anode and OH^- at the cathode and the electrophoretic migration of these ionic products, strong pH gradients between the electrodes may be expected in electrofiltration.

Changes in pH during electrofiltration may also affect the electrokinetic effects and thus the electrofiltration rate. Usually, the electrodes used in electrofiltration are made from insoluble materials (such as precious metals, conductive ceramics). However, in case soluble anodes are used (such as aluminum or iron), anode electrolysis generates ions that can be very effective in the coagulation of the suspended particles (Larue et al., 2003). The coagulation effect induced by pH or by other electrolytic products may increase the filter cake permeability and help the filtration process. Also, the electrolyte resistance generates heat that may be important during electric current flow. The temperature increase in the suspension reduces its viscosity, thus facilitating mechanical dewatering (Weber and Stahl, 2002). Depending on the nature of the particles, gravitational sedimentation may also have an effect, especially in horizontal filters (automatic filter press, leaf, belt press). Some researchers have shown that neglecting sedimentation flux in ordinary filtration leads to an underestimation of the amount of solids deposited in the cake compared to the amount predicted by conventional filtration theory (Bockstal et al., 1985; Iritani et al., 1999; Tiller et al., 1995; Wakeman, 1981). For these reasons existing mathematical electrofiltration models taking into account hydrodynamical and electrokinetic effects only must be further extended (Iritani et al., 1992; Yukawa et al., 1976).

The objective of this article is the investigation of combined influences of side effects such as water electrolysis, gas formation, and particle sedimentation. This report introduces a mathematical model, incorporating some side effects, to describe the electrofiltration rate, based on the views of Jujikov (1971), Tiller et al. (1995), Biesheuvel and Verweij (1999), Iritani et al. (1992), and Vorobiev et al. (1999). The conditions of applicability and the limits of this theoretical model are defined from tests on a constant pressure laboratory horizontal filter filled with a kaolin suspension. The contributions of sedimentation, heat production, and electrolysis products are established. The evolution of pH inside the filter attributed to water electrolysis in electrofiltration is yet to be studied.

Theoretical Analysis

In the theoretical analysis of electrofiltration, the filter cake is assumed to be incompressible and the liquid is modeled as Newtonian. In a first attempt, a gravitational sedimentation term is introduced in the existing electrofiltration model. Before considering the electrofiltration process, it is useful to discuss the settling effect in filtration. A sketch of a filter cell is shown in Figure 1A, where one observes that the filtration on the horizontal surfaces facing upward is accompanied by sedimentation. A constant pressure is applied at the top of the suspension at an original height H_0. A filter cake of thickness δ is formed on the filter surface. The location of the top surface of the suspension is given by H and the region represented by

$H_0 - H$ equals the volume of filtrate/unit area v. Particles with density greater than the liquid density settle under the effect of gravity. As the filtrate flows down, the solids are driven down with a velocity greater than that of surrounding liquid because of difference in density. In the case of real suspensions where particles have various sizes, settling large particles are interspersed with smaller particles. A point is reached where presumably all particles have the same velocity and settle down as a "zone" of height H_S. A supernatant free of particles may appear between the top surface of the suspension (at height H) and the top surface of the sediment zone at height H_S. The propagation velocity of the supernatant zone (between H and H_S) represents the relative settling velocity, $u_{SR} = u_S - u_L$, where u_S and u_L are the solid and liquid velocities, respectively. This velocity is closely related to the volumetric concentration ϕ_S of the suspension (Kynch, 1952). The relative settling rate decreases with increasing volumetric concentration ϕ_S.

In agitated suspensions, settling is of secondary importance ($u_{SR} \sim 0$) and the dewatering rate is adequately described by the Ruth parabolic relationship (Ruth, 1946). For significant u_{SR} values, the rate of solids deposition on the horizontal medium will be underestimated and errors will be introduced in the relationship of the volume of filtrate with time (Bockstal et al., 1985; Wakeman, 1981). If the $(H_S - \delta)$ settling zone is assumed to be ideal (for a constant concentration ϕ_S), the relative sediment velocity u_{SR} will be constant. This will provide a reasonable predictive power for a large range of conditions (Biesheuvel and Verweij, 1999; Tiller et al.,1995). The height of the interface H_S can then be related to the piston height H and the filtration time t by

$$H_S = H - u_{SR}t \qquad u_{SR} \geq 0 \tag{1}$$

When an electric field of intensity E is applied, as shown in Figure 1B, a change in the relative settling velocity of particles will occur. Figure 1B shows the filter cell equipped with electrodes. The anode is in contact with the top surface of suspension at an initial height H_0. The cathode is placed against the horizontal filter surface. In the presence of negatively charged particles, this setup will enhance the electrofiltration rate by both electrophoresis and electroosmosis. In addition to mechanical pressure, electroosmotic pressure helps to accelerate the filtration. Charged particles are electrophoretically attracted toward the anode. This hinders the cake buildup and minimizes its resistance to downward liquid flow. Free particles subjected to an electric field only acquire an electrophoretic velocity u_E given by the product of the field strength E and the electrophoretic mobility k

$$u_E = kE \tag{2}$$

In the configuration of Figure 1B, the gravitational sedimentation offsets the electrophoretic force. For the same filtrate volume, the sediment height in the presence of electric field H_{SE} will be higher than the sediment height in the absence of electric field, $H_{SE} > H_S$. Therefore, the cake thickness δ_E obtained from electrofiltration will be smaller than the filter cake thickness δ obtained from conventional filtration. The particle settling velocity in an electric field may be estimated from the difference between the relative settling velocity in ordinary filtration u_{SR} and the electrophoretic velocity u_E defined previously. If the settling zone within $(H - H_{SE})$ is assumed to be ideal (for a constant concentration ϕ_S), the particle settling velocity is constant and the location of the sediment height H_{SE} is given as

$$H_{SE} = H - (u_{SR} - u_E)t \qquad u_{SR} \geq 0,\ u_E \geq 0 \tag{3}$$

Simple application of mass conservation to the solid phase can relate the quantities involved in Figure 1A or 1B as follows

$$\phi_S H_0 = \phi_S(H_S - \delta) + \phi_C\delta \qquad \text{with } E = 0$$

$$\phi_S H_0 = \phi_S(H_{SE} - \delta_E) + \phi_C\delta_E \qquad \text{with } E > 0 \tag{4}$$

where ϕ_C is the solids concentration of the cake given by $\phi_C = 1 - \varepsilon$, where ε is the cake porosity. All variables in the previous equations can be obtained from experiment.

Mathematical model of electrofiltration

The introduction of a mathematical model to describe electrofiltration is useful to point out the significance of electrokinetic effects as compared to sedimentation. A differential mass balance may be written for the filter medium, where the growth rate of the filter cake is expressed as a function of v, the volume of filtrate/unit area

$$\frac{dw}{dt} = c_0\frac{dv}{dt} + \phi_S\rho_l(u_{SR} - u_E) \qquad u_{SR} \geq 0,\ u_E \geq 0 \tag{5}$$

where w is the mass of dry cake/unit filter area, c_0 is the mass of solids/unit of filtrate volume in ordinary filtration, and ρ_l is the density of the suspension. In the right-hand side of Eq. 5, the first term is the mass flux of solids transported by convection up to the filter cake. The second term is the mass flux of solids deposited on the filter cake by sedimentation in presence of a DC electric field. The filtration rate continually decreases as the size of the filter cake grows. If the transport of solids away from the cake by electrophoresis equals the filtration and sedimentation transport, then $dw/dt = 0$ and the filter cake ceases to grow. In such an equilibrium condition, the dynamically balanced filtration rate q_{SE}, derived from Eq. 5, is given as

$$q_{SE} = \frac{\phi_S\rho_l(u_E - u_{SR})}{c_0} \tag{6}$$

With the exception of the equilibrium condition of Eq. 6, the electrofiltration flow rate q may be expressed as the sum of two components: the hydraulic flow and the electroosmotic flow through the filter cake. If the total flow rate is consistent with Darcy's law, it may be written as a two-resistance (R_C = cake, R_m = supporting medium) model in the form (Iwata et al., 1991)

$$q = \frac{dv}{dt} = \frac{\Delta P + \Delta P_E}{\mu(R_c + R_m)} = \frac{\Delta P + \Delta P_E}{\mu(\alpha_{av}w + R_m)} \tag{7}$$

where ΔP is the filtration pressure and ΔP_E is the electroosmotic force/unit filter area. The cake resistance is given by the product of the average specific cake resistance α_{av} and w, the mass of solids/unit filter area. Integrating Eq. 5 and substituting it into the Eq. 7 yields

$$q = \frac{dv}{dt} = \frac{\Delta P + \Delta P_E}{\mu[\alpha_{av} c_0 (v - q_{SE} t) + R_m]} \tag{8}$$

Solving Eq. 8 with the initial condition $v = 0$ at $t = 0$, a constitutive expression of electrofiltration with sedimentation relates the time to the volume of filtrate

$$t = \frac{v}{q_{SE}} + \left(\frac{K_E}{2q_{SE}^2} - \frac{v_{eq}}{q_{SE}}\right) \times \left[\exp\left(-\frac{2}{K_E} q_{SE} v\right) - 1\right] \qquad \text{with } q_{SE} \neq 0 \tag{9}$$

where K_E and v_{eq} are constants defined as

$$K_E = \frac{2(\Delta P + \Delta P_E)}{\mu \alpha_{av} c_0} \tag{10}$$

and

$$v_{eq} = \frac{R_m}{\alpha_{av} c_0} \tag{11}$$

It is worth noting that the expression given in Eq. 9 may be used as a generalized constitutive equation in three processes: electrofiltration with sedimentation (EF + S) or electrofiltration without sedimentation (EF) and ordinary filtration with sedimentation (F + S). In the EF process, $u_{SR} = 0$ and $q_{SE} = q_{E0} = \phi_S \rho_l u_E / c_0$ in Eq. 6; then Eq. 9 reduces to the expressions developed by Iritani et al. (1992) with a negligible medium resistance (R_m, $v_{eq} \sim 0$) and by Vorobiev et al. (1999) with significant medium resistance. In the (F + S) process, $u_E = 0$, $\Delta P_E = 0$, and the coefficient K_E can be defined in the absence of electric field as

$$K_E = K_0 = \frac{2\Delta P}{\mu \alpha_{av} c_0} \tag{12}$$

If $q_{SE} = q_{S0} = -\phi_S \rho_l u_{SR} / c_0$ is substituted into Eq. 6, Eq. 9 takes a form expressed for the (F + S) process by Jujikov (1971), Bockstal et al. (1985), Tiller et al. (1995), or Biesheuvel and Verweij (1999). Finally, if there is no electric field and no sedimentation ($q_{SE} = 0$) then Eq. 9 is no longer valid. In this case, the t/v vs. v curve is usually a straight line according to the classical Ruth equation of filtration. This equation can be written using the previously introduced coefficients K_0 and v_{eq} as

$$\frac{t}{v} = \frac{1}{K_0}(2v_{eq} + v) \tag{13}$$

In ordinary filtration, the deviation from linearity in Ruth's t/v vs. v plot may be indicative of transient behavior (interacting species, flocculation, hydraulic flow patterns, particle migration, and deposition) (Wakeman and Tarleton, 1998).

Constant Rate Stage

After all solids have been deposited by sedimentation on the surface of filter cake, that is, when the height of sediment is $H_S = \delta$ in Figure 1A or $H_{SE} = \delta_E$ in Figure 1B, pure liquid flows through the cake by permeation. The transient zone between the sedimentation and permeation regime must be carefully defined in the experiments. In the permeation stage, if the filtration pressure does not change, the liquid flow is linear in time for incompressible cakes and the cake resistance remains constant. In the presence of an electric field, the filtrate flow rate q is the combination of the flux q_p caused by the constant pressure force and the constant electroosmotic flux q_E (Iwata et al., 1991; Yukawa et al., 1971). The flow rate q is derived from Darcy's law with $R_m \cong 0$ ($R_m \ll R_C$), as follows:

$$q = \frac{dv}{dt} = q_p + q_E \tag{14}$$

where the constant flow rates q_p and q_E are given as

$$q_p = \frac{\Delta P}{\mu \alpha_{av} w} \qquad \text{and} \qquad q_E = \frac{\Delta P_E}{\mu \alpha_{av} w} \tag{15}$$

Solving Eq. 14 with the initial condition $v = 0$ at $t = 0$ yields an expression relating v to time for the process of permeation (P) or electrical permeation (EP) of liquid through the filter cake

$$t = \frac{1}{q} v + \beta \qquad \text{with } q = q_p \text{ if } E = 0 \tag{16}$$

where β is a constant. If the cake is compressible, some cake deformation is expected when solids cease to deposit on its surface. This would lead to an increase in the cake resistance and a decrease in the total filtrate flow rate q. However, under most conditions encountered in practice, it is unlikely that q varies more than 10–20%. The variation is small for dilute suspensions with slow rates of cake buildup (Tiller et al., 1995).

Electrolysis reactions at the electrodes

Predictive models may be effective in the early stages of electrofiltration. However, side effects such as the suspension heating, generation of electrolysis products, and the variation of hydraulic cake permeability may significantly influence the behavior of the process. When an electric field is applied, the electrolyte electrical resistance generates heat. A subsequent increase in temperature reduces viscosity and mechanical dewatering is facilitated. This decrease in viscosity may be inferred from the temperature T inside the filter cake using data from the literature (Cho et al., 1999). Voltages used in electrofiltration usually exceed the decomposition voltage of water. In case insoluble electrodes are used (precious metal, carbon,

ceramics), water electrolysis reactions take place at the electrodes and generate gases and ionic products as follows

$$\text{Anode:} \quad 2H_2O - 4e^- \rightarrow 4H_3O^+ + O_{2(g)}$$

$$\text{Cathode:} \quad 2H_2O + 2e^- \rightarrow 2OH^- + H_{2(g)}$$

The amount of each electrolysis product, n_p, according to Faraday, is proportional to the product of current intensity I and the time of applied current

$$n_p = \frac{\lambda I t}{nF} \tag{17}$$

where λ is the stochiometric coefficient of the electrolysis reaction, n is the amount of electron moles, and F is the Faraday number (96,500 coulombs). In the configuration of Figure 1B, gases that accumulate at the anode can improve the filtrate flow rate by displacing the suspension. The gas contribution to electrofiltration can be integrated in the volume of filtrate/unit area v introduced in previous electrofiltration models, as follows

$$v = H_0 - H + n_p v_{mol} \tag{18}$$

where v_{mol} is the molar volume of gas/unit filter area. The amount of gas generated should be carefully controlled; otherwise, the electrical contact between the anode and the suspension can be affected by the presence of an electrically isolating layer of gas around the anode. At the end of filtration, the gases accumulated have a rather positive role because they are stored in the cake, whereby the cake is no longer saturated and the residual moisture is reduced (Weber and Stahl, 2002). Although the above water electrolysis reactions show that OH^- and H_3O^+ ions are generated in equal quantities, drastic changes of pH are expected during electrofiltration. In the context of Figure 1B, a cation flow is created in the downward direction. Because the particles used in the experiments have negative ζ-potential, H_3O^+ cations are actually electroosmotically drained by the filter cake with a velocity q_E, which can be derived from the modified Helmholtz–Smoluchowski equation

$$q_E = \frac{D\varepsilon\zeta E}{\mu} \tag{19}$$

where D is the permittivity of water and E is the electric field intensity through the filter cake. Despite the downward direction of the cation flow, an accumulation of anodic H_3O^+ cations will cause a probable pH decrease in the suspension and inside the upper layers of the cake.

Meanwhile, the part of the filter cake near the cathode becomes alkalified because OH^- ions are attracted by the anode. Therefore, the pH through the cake would not be uniform during the electrofiltration process. If the original pH is nearly neutral throughout the cake, a pH gradient would appear. The cake becomes basic at the cathode and acidic near the suspension. This result was verified by Yoshida et al. (1999) for the electrodewatering process of semisolid materials and by Bazhal and Vorobiev (2000) for electrodewatering of biological materials. As in most suspensions, the ζ-potential of the particles is pH dependent. According to Eq. 19, a growth of pH distributions inside the cake can affect the electrofiltration rate. The pH decrease above the filter cake will even have an effect on the electrophoretic mobility of particles, k, depending on the particles' ζ-potential, as indicated in the approximation of Smoluchowski (Lyklema, 2003)

$$k = \frac{\zeta D}{\mu} \tag{20}$$

In electrofiltration, it is important to define the pH evolution because it has a significant impact on the ζ-potential of particles, and thus on the electrofiltration rate.

Materials and Methods

Electrofiltration experiments were carried out in a filter module with glass transparent walls built in the laboratory. The dimensions of the cylindrical feed chamber are 13×3.25 cm with an effective filter medium area of 8.33 cm^2. Figure 1 shows a schematic view of the filter chamber. The suspension is introduced in the chamber up to height $H_0 = 8.7$ cm (corresponding to a filter volume of 72.5 mL) at ambient temperature (20°C). Constant pressure (0–120 kPa) was applied at the top of the suspension by a Teflon piston. A paper filter medium (retention capacity: 8 μm; Whatman) was placed at $H = 0$ cm above a cathode mesh in steel. The cathode is placed on a Teflon support, perforated to allow for the transfer of filtrate to a collecting vessel. The anode is a titanium plaque mounted flush with the piston. The electrodes were connected to a DC power supply (Consort E861) delivering a constant current intensity with a maximum of 80 mA (1 A/dm^2 of electrode surface). Experiments were monitored by a PC through an IEEE interface. Parameters sampled by the computer are the height of the piston H, the voltage, and the current intensity. The electric field intensity is obtained by dividing the voltage by the electrode spacing. The level of settling zone interface, H_S ($E = 0$) or H_{SE} ($E > 0$), is measured visually from within the filter module through its transparent walls. At the end of each experiment, the cake thickness is measured and the wet cake is desiccated in an infrared desiccator (Scaltec SMO 01) to determine the ratio of wet to dry cake mass m. The cake concentration ϕ_C (solidosity) is then calculated as

$$\phi_C = \frac{\rho_l}{\rho_S(1/m - 1) + \rho_l} \tag{21}$$

The temperature inside the filter cake is measured during electrofiltration using a thermocouple attached to the filter paper. Some tests required stirring the suspension. Low constant agitation (at 100 rpm) is provided by a magnetic stirrer bar placed inside the filter cell at 2 cm above the filter medium. In all experiments, kaolin particles (Kerbrient SP20; density $\rho_S = 2600$ kg/m^3) were dispersed in NaCl solution (0.02 mol/L) with a solid volumetric concentration $\phi_S = 0.015$ in a range of pH adjusted using HCl or NaOH. The mean size of kaolin particles was measured by a Mastersizer X (Malvern Instru-

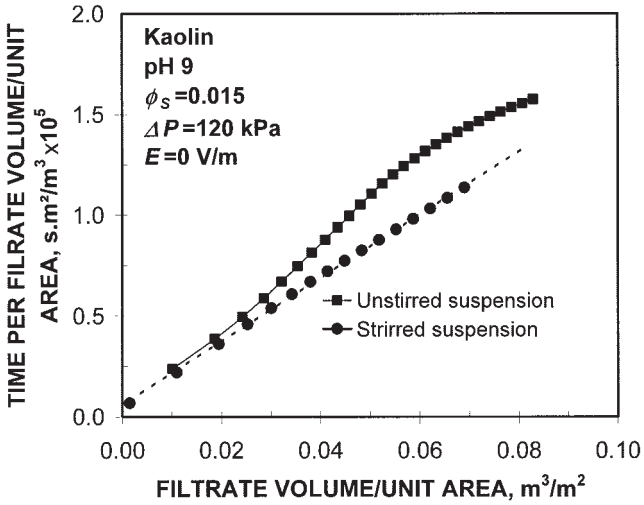

Figure 2. Ruth diagram of filtration with and without agitation under constant pressure in the absence of electric field.

ments, Worscestershire, U.K.) and revealed a polydisperse size distribution with a median size of 13.7 μm.

Analysis of Experimental Data

Characterization of the parameters in the empirical constitutive relations was accomplished by fitting experimental t–v data to theoretical formulas using the data-fitting software Table Curve 2D. Heat, gas production, and pH evolution during electrofiltration were analyzed for several electric field magnitudes. An attempt was made to quantify their contribution to the electrofiltration process. As a result, the limit of applicability of the electrofiltration model was established. If the coefficients q_{SE}, K_E, and v_{eq} of Eq. 9 are unknown, the fitting of Eq. 9 with electrofiltration data provides a multitude of solutions. Knowledge of at least one of these coefficients is required to determine a unique correlation result. Herein, the approach adopted is to fix the q_{SE} value that can be derived from the relative sediment velocity. Before the current is applied, data from ordinary filtrations were collected to assess the validity of approximations used in the basic theory (filter cake incompressibility and the constant relative settling velocity) and the applicability of theoretical formulas to the filtration flow rate. The filter medium resistance, the specific cake resistance, and the relative settling velocity were then determined and incorporated into the electrofiltration model. Finally, the characterization of q_{SE}, K_E, and v_{eq} is achieved for the electrofiltration process and all the factors controlling the electrofiltration rate (specific cake resistance, settling velocity, electrophoretic velocity, electroosmotic pressure) are defined.

Relative settling velocity

Representative results depicting the filtration with stirred or unstirred suspensions at pH 9 in the absence of electric field are shown in Figure 2. After introducing the suspension into the filter, the piston pressure was adjusted to the constant value of 120 kPa, and cake deposition on the horizontal surface ensued. Figure 2 presents Ruth plot data, in t/v vs. v coordinates. In this diagram, the filtration of stirred suspension is represented by a straight line indicating rapid cake buildup and a filter medium dominated by cake resistance. A marked deviation from linearity is noticed for filtration with unstirred suspension. Sedimentation is usually the cause of this extra resistance in addition to what is predicted by Ruth's equation. From the transparent walls of the filter cell, three interfaces could be visually discerned. These interfaces are located at the sediment height H_S, piston height H, and cake thickness δ.

In Figure 3, these data are shown for the filtration with unstirred suspension. The distance $H_0 - H$ equals the filtrate volume/unit area v. At the time $t = 0$ (point A), the sediment height H_S coincided with the piston height H. The solids settled simultaneously, forming a horizontal interface with clear liquid above it in the zone between H and H_S. The distance $H - H_S$ represents the product of the relative settling velocity and time, $u_{SR} \times t$. When H_S reached point C in Figure 3, all of the solids have settled out, and cake formation is completed. Clear liquid then flowed through the cake by mechanical permeation and the cake thickness remained constant at $\delta = 4$ mm. At the end of the process, the measured solid concentration in the cake was $\phi_C = 0.34$ (porosity $\varepsilon = 0.66$). It can be concluded that the studied kaolin suspension is not easily filterable (total filtration time $\cong$ 13,000 s at point D). This is attributed to the relative electrostatic stability of kaolin particles ($\zeta \cong -8$ mV). The relative settling velocity was not uniform along path AC.

In determining the relative settling velocity for the runs shown in Figure 3, a deviation from linearity in a $(H - H_S)$ vs. t plot occurred and was particularly severe at approximately $t = 2000$ s (at point E). The resulting decrease in velocity is characteristic of batch sedimentation (Kynch, 1952) or filtration with sedimentation (Tiller et al., 1995). When the cake is formed, stresses are transmitted from the cake surface through points of contact between the particles. A gradual compression of particles in the EC path leads to a progressive decrease in settling velocity. Because the electrofiltration model is based on a constant settling velocity, an approximation was required.

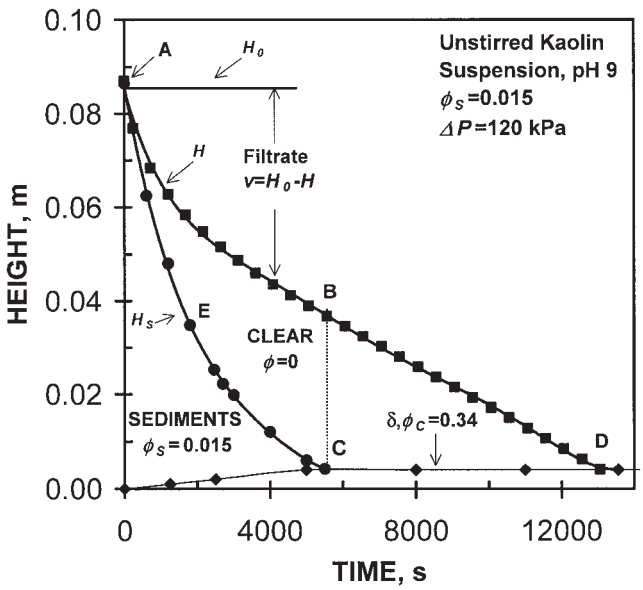

Figure 3. Filtration with sedimentation under constant pressure in the absence of electric field.

Table 1. Results of Correlation between Theoretical Equations and Filtration Data

	Correlated Coefficients			Filtration Parameters	
Filtration Period*	$K_0 \times 10^{-7}$ ($m^2\ s^{-1}$)	$v_{eq} \times 10^{-3}$ ($m^3\ s^{-2}$)	$q_P \times 10^{-6}$ ($m\ s^{-1}$)	$R_m \times 10^{11}$ (m^{-1})	$\alpha_{av} \times 10^{12}$ ($m\ kg^{-1}$)
F (Eq. 13)	6.5 ± 0.3	2.1 ± 0.8		7.7 ± 2.7	9.6 ± 0.6
F + S (Eq. 9)	6.8 ± 0.3	2.5 ± 0.8		8.6 ± 2.5	9.1 ± 0.4
P (Eq. 16)			3.9 ± 0.2		9.1 ± 0.4

*F, filtration with stirred suspension; F + S, filtration with sedimentation; P, filtration at constant rate period.

As suggested by Tiller et al. (1995), an estimation of the settling velocity can be obtained by locating B (Figure 3), the point at which the H vs. t relation becomes linear. Assuming that the cake thickness at point C is known, the distance BC can then be calculated and divided by t_S (time at point B or C) to obtain u_{SR}. The relative settling velocity at the point C can then be given as

$$u_{SR} = [H(t_S) - \delta]/t_S \tag{22}$$

where $H(t_S)$ is the piston height at time t_S. The value of u_{SR} calculated in this way should be representative of the average flux of solids deposited onto the cake surface during the overall period of the settling process. In this procedure, the relative settling velocity calculated by means of Eq. 22 with $t_S \cong 5500$ s yields a relative settling velocity $u_{SR} = (6.1 \pm 0.2) \times 10^{-6}$ m/s for five runs identical to that of Figure 3.

Filter medium and filter cake resistances

Three theoretical equations can be used to describe the filtration behavior of the previously described runs. Because the t/v vs. v curve in Figure 2 is a straight line for filtration with agitation (F process), the Ruth equation Eq. 13 can successfully be used to describe the filtration flow rate. Two periods can be distinguished during the filtration of the unstirred suspension. In the first period, for $t < t_S$, the settling takes place and it can be inferred from Figure 3 that the t vs. v plot has an exponential form (F + S process, line AB). The filtrate flow can then be described by Eq. 9 knowing the value of q_{S0} in the absence of the electric field. In Eq. 6, the approximation $\phi_S \rho_l \cong c_0$ for the dilute kaolin suspension ($\phi_S = 0.015$) yields $q_{S0} \cong -u_{SR}$ ($= -6.1 \times 10^{-6}$ m/s). In the second period, for $t > t_S$, the particles ceased to settle and liquid flowed through the cake by permeation at constant rate (P process, line BD in Figure 3). The filtration data in the t vs. v plot can then be described by Eq. 16. The filtration data were accurately fit to the theoretical model using Table Curve 2D software (with a correlation coefficient: $0.999 < R^2 < 1$).

Table 1 details the correlated K_0, v_{eq}, and q_p parameters entering in Eqs. 9, 13, and 16. Values given in Table 1 are averaged with standard errors for five identical runs. The K_0 coefficient and the specific cake resistance α_{av} in the (F) and (F + S) processes were calculated from Eq. 10. The permeation flux q_P in the (P) process and the α_{av} value are obtained from Eq. 15. In all these calculations, the viscosity is $\mu = 0.001$ Pa·s, the pressure is $\Delta P = 120$ kPa, and the mass of solids/unit of filtrate volume c_0 is $\rho \times \phi_S = 38.5$ kg/m^3. The value of filter resistance R_m was subsequently obtained from Eq. 11 using the v_{eq} and α_{av} values previously calculated. The filter resistance was rather small compared to cake resistance ($R_C = \alpha_{av} \times w = 3.1 \times 10^{13}\ m^{-1} \gg R_m$), where w ($= H_0 \times c_0 = 3.36$ kg/m^2) is the mass of dry solids/unit area. As shown in Table 1, the α_{av} and R_m values obtained for the (F), (F + S), and (P) processes are close, indicating that the filtration models seem to account rather well for the experimental results. This corroborates the analysis of Jujikov (1971), who established that the settling effect did not change the specific cake resistance. Therefore, the determination of relative settling velocity from Eq. 22 and the use of $q_{S0} \cong -u_{SR}$ in Eq. 9 constitute a priori valid approximations in the description of the sedimentation effect.

The extent of compressibility of the kaolin cake was investigated. Filtration data of stirred suspensions at constant pressures of 60, 90, and 150 kPa were treated in the t/v vs. v plot using Ruth's Eq. 13. Assuming that the specific cake resistance is a power function of the pressure, the following empirical equation emerged

$$\alpha_{av} = 5.4 \times 10^{11} \Delta P^{0.25}\ (\text{m/kg}) \tag{23}$$

The value of the exponent is reasonable for kaolin suspensions. Equation 23 displays a low compressibility coefficient of 0.25, indicating the relative incompressibility of the filter cake. Therefore, the approximation of the filter cake as an incompressible solid in the basic theory is reasonable for kaolin suspensions.

ζ-Potential of particles

The ζ-potential of the particles was defined as well as its dependency on pH. A fixed bed of kaolin particles was created by filtration of unstirred suspension. During the period of constant rate of filtration a constant current was applied at $t =$ 8000 s that generated an electroosmotic flow q_E in addition to the mechanical dewatering flow q_p. Figure 4 shows the filtrate volume/unit area obtained as a function of time before and after a current was applied to a suspension at pH 9. Various constant currents (0.2, 0.3, 0.5, and 1.0 A/dm^2) were briefly tested so that the pH, the temperature of the suspension and the electric field intensity remain unchanged. As shown in Figure 4, with the current applied, the t vs. v curve remained a straight line but with a reduced slope, indicating that the total flow rate q ($= q_P + q_E$) was increased. The total flow rate and therefore the electroosmotic flow rate were improved by an increase in current intensity. The slope of the lines before and after current application provided the values of q_p and q, respectively. The difference $q - q_P$ that yields the value of electroosmotic flow rate is listed in Table 2 for each current intensity. Knowing the electroosmotic flow rate, the ζ-potential of the particles was obtained from the Helmholtz–Smoluchowski formula in Eq. 19 using $\mu = 0.001$ Pa·s, $\varepsilon = 0.66$, and $D = 6.94 \times 10^{-10}$ F/m; Eq. 19 yields ζ (pH 9) $= -8.1 \pm 1$ mV. The previously

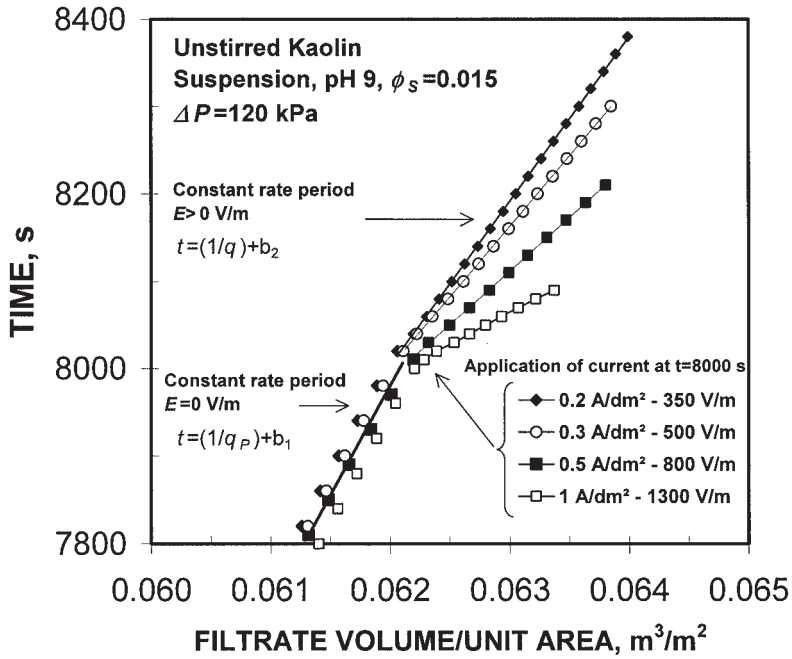

Figure 4. Application of several constant currents in the constant filtration rate period without agitation.

described testing procedure was repeated for suspensions with pH values ranging from 2 to 11. Figure 5 shows that the particles' ζ-potential increases as the pH decreases. An isoelectric point (IEP) occurred at pH $\approx$ 2 that coincided with a flocculation of kaolin particles. The settling velocity of the flocculated particles at pH 2 is estimated from Eq. 22 to be twice the value found at pH 9. The specific cake resistance was reduced from 9.1×10^{12} m/kg at pH 9 to 3.3×10^{12} m/kg at pH 2.

Influence of pH changes in electrofiltration

Typical results from an electrofiltration at 0.5 A/dm^2 with unstirred suspension at pH 9 are presented in Figure 6. Electrofiltration is preceded by a 2100-s filtration period to draw the electrodes close together, thus minimizing the ohmic heating when the current is applied. Figure 6 shows the evolution of the piston height H, the sediments height H_S (with $E = 0$) and H_{SE} (with $E > 0$), and cake thicknesses δ (with $E = 0$) and δ_E (with $E > 0$). With the current applied at $t_0 = 2100$ s (point B), the curvature of the H vs. t graph decreases, exhibiting an enhanced electrofiltration rate compared to filtration before t_0. The electrophoresis force that tends to move particles toward the upper electrode did not prevent settling of the particles; the solids formed a horizontal interface with a clear liquid above them in the zone between H and H_{SE}. The distance $H - H_{SE}$ represents the product of the relative settling velocity and the time, $(u_{SR} - u_E) \times t$. The relative settling velocity in electrofiltration should be lower compared to that involved in ordinary filtration. Surprisingly, this was not the case. At point F, solids have settled out and cake formation is complete. The estimated relative settling velocity at point F from Eq. 22 was 6.5×10^{-6} against 6.1×10^{-6} m/s in ordinary filtration.

A particular phenomenon occurred in the time interval $t_0 + 1500$ s $< t < t_0 + 2000$ s, where t_0 is the time of current application ($t_0 = 2100$ s). During this time, a sudden change in electrofiltration rate is observed (between points C and D; Figure 6). It was associated with a significant growth in cake thickness, from 3.5 mm ($t_0 + 1500$ s) to 5.5 mm ($t_0 + 2000$ s), and a decrease in H_S vs. t curvature. This result cannot be explained by the temperature increase only, which was 6°C at $t_0 + 1500$ s.

To investigate the observed effect, electrofiltration runs were conducted at 0.5 A/dm^2 using the previously described procedure. However, these runs were stopped at various times to collect the clear liquid in the vicinity of the anode, the filtrate, and filter cake (including sediments). The pH measurements in these different systems clearly identify the OH^- and H_3O^+ ions generated by water electrolysis as causing this drastic

Table 2. Results of Correlation between Theoretical Equations and Electrofiltration Data*

	EP (Eq. 16)		EF + S (Eq. 9)		EF (Eq. 9)	
Current (A/dm^2)	$q_E \times 10^{-6}$ (m s^{-1})	$\Delta P_E \times 10^5$ (Pa)	$K_E \times 10^{-6}$ (m^2 s^{-1})	$\Delta P_E \times 10^5$ (Pa)	$K_E \times 10^{-6}$ (m^2 s^{-1})	$\Delta P_E \times 10^5$ (Pa)
0.2	1.4	0.42	0.88	0.35	0.88	0.35
0.3	2.2	0.69	1.04	0.63	—	—
0.5	3.9	1.20	1.38	1.22	1.40	1.25
1.0	5.7	1.72	2.00	2.30	2.00	2.30

*EF, electrofiltration with stirred suspension; EF + S, electrofiltration with sedimentation; EP, electrofiltration at constant rate period.

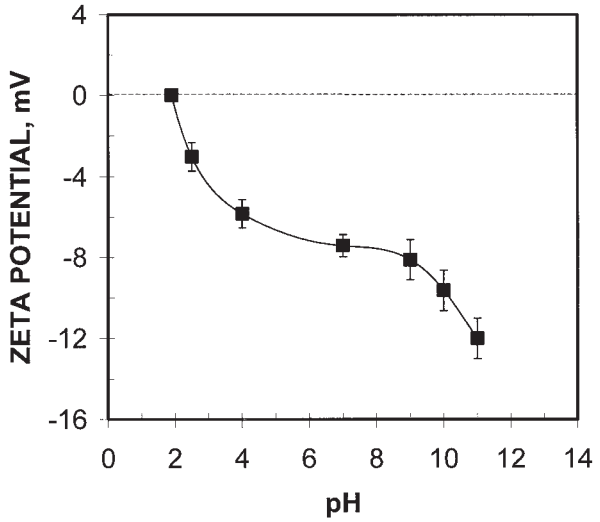

Figure 5. ζ-Potential of kaolin particles, pH adjusted with either HCl or NaOH.

change in electrofiltration behavior. As shown in Figure 7, a decrease in pH from 9 at time t_0 to 1.9 at time $t_0 + 2400$ s is observed in the clear liquid collected near the anode. It can be assessed that the IEP (pH ≅ 2) corresponding to flocculation of kaolin particles was reached at time $t_0 + 1500$ s. A part of OH^- ions generated by cathode electrolysis was removed and the filtrate became alkalified as a result of downward liquid flow. The pH in the filter cake and sediments above it became even more alkalified as the electrofiltration progressed as a result of OH^- ions migrating toward the anode (Figure 7). There was probably a distribution of pH inside the cake, typical of the electrodewatering process (Yoshida et al., 1999). The pH gradually decreased from a basic pH at the cake side adjacent to the cathode to an acid pH in the upper layers of the sediments. During electrofiltration, a decrease in cake pH occurred at approximately $t_0 + 1500$ s.

This moment coincides with the onset of IEP near the anode and with an abrupt increase in electrofiltration rate in Figure 6. Therefore, it can be assumed that the IEP occurring near the anode reached the upper layers of the cake and propagated through it. This resulted in particle coagulation inside the filter cake. This coagulation effect was corroborated by a decrease in the cake concentration from $\phi_C = 0.34$ for $t_0 + 1000$ s (before IEP zone) to $\phi_C = 0.24$ for $t_0 + 2000$ s at point F. A lower cake concentration is actually characteristic of the coagulation effect that tends to increase the cake moisture and thickness. The resulting higher cake permeability facilitated the electrofiltration, as shown in Figure 6, when the whole cake is close to IEP (at point D, Figure 6); the potential V decreased and the electroosmotic flow rate decreased in accordance with Eq. 19. Consequently, the electrofiltration rate decreased again. Clear liquid acid then flowed through the cake in the electrowashing mode.

The coagulation of the particles inside the filter cake is potentially interesting for the use of electric field. The previous run was repeated and electrofiltration was stopped before and after IEP, at $t_0 + 1000$ s and $t_0 + 2400$ s, as shown in Figure 8, where t is plotted vs. v. Subsequently, filtration at the same constant pressure was restarted. After the current was applied for 1000 s (pH near anode: 2.3), the filtration was restarted in ordinary filtration mode; the slope of t vs. v increased sharply and the specific cake resistance increased to $\alpha_{av} = 9.1 \times 10^{12}$ m/kg. After the current was applied for 2400 s (pH near anode: 1.85), the filtration was restarted at an increased flow rate close to that of electrofiltration ($\alpha_{av} = 3.2 \times 10^{12}$ m/kg). This increase is mainly caused by the coagulation effect in the filter cake. Consequently, for a limited electrical treatment, the over-

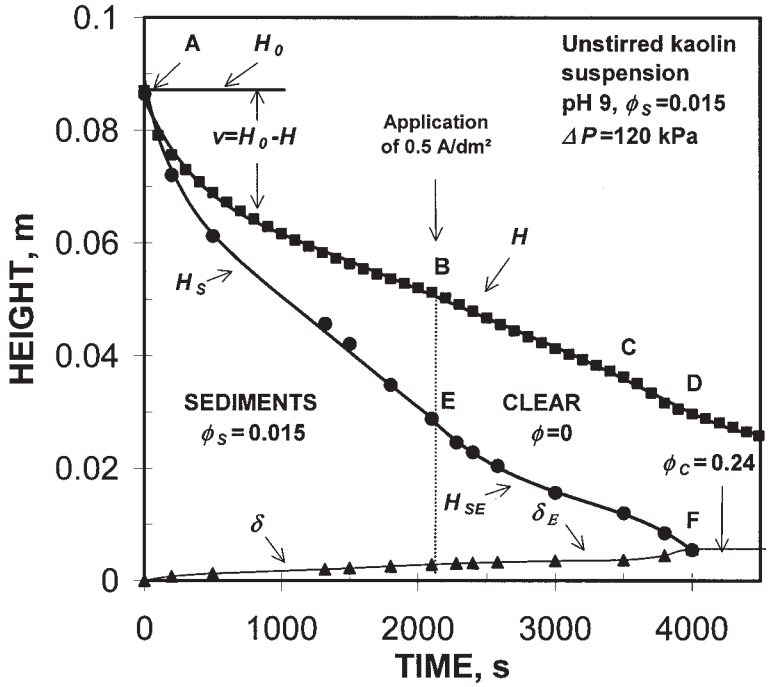

Figure 6. Typical electrofiltration with sedimentation under constant pressure at 0.5 A/dm².

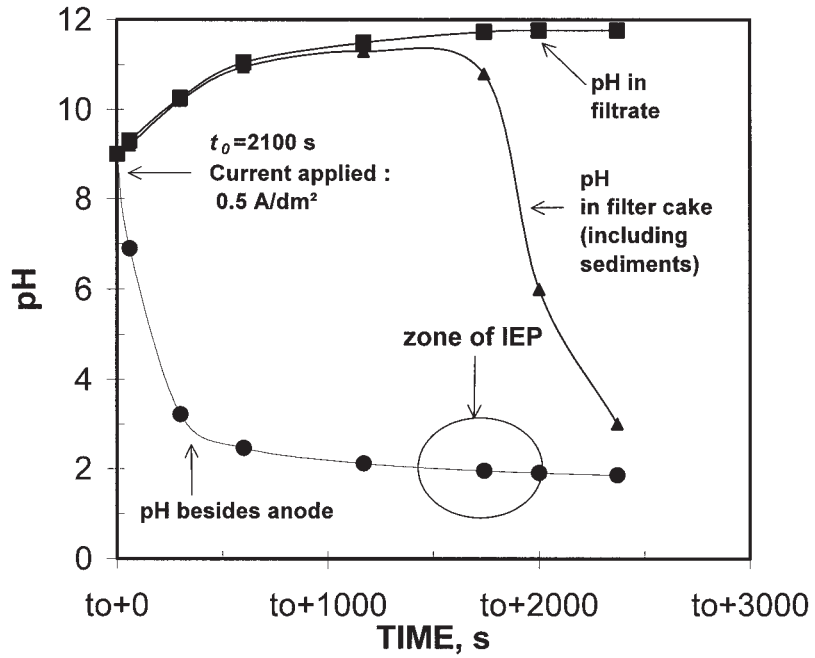

Figure 7. pH history of suspension filter cake and filtrate during electrofiltration.

all processing time was significantly reduced. Moisture was increased in the coagulated cake by a short cake expression (≈100 s) at the end of process. The electrolytic gases accumulated at the anode side helped displace the cake water and restore its concentration to $\phi_C = 0.34$. After 2400 s of applied current, the filtrate's pH was 11.75 and the subsequent mechanical permeation of liquid acid at pH 1.85 brought it back down to pH 10.6 at the end of the process.

The coagulation phenomenon deserves further attention because different mineral suspensions are highly pH dependent and could be amenable to coagulation using the electrofiltration process. It would not be necessary to apply the DC electric field during the entire filtration process but only within a specific window of time during which the isoelectric point leading to coagulation of particles is reached. The significant increase in cake permeability and reduction of the filtrate viscosity resulting from the heat production allow for subsequent filtration at a rapid rate. This may provide substantial savings in energy requirements compared to a full-time electrofiltration. Furthermore, just like electrodialysis, this process could be used to

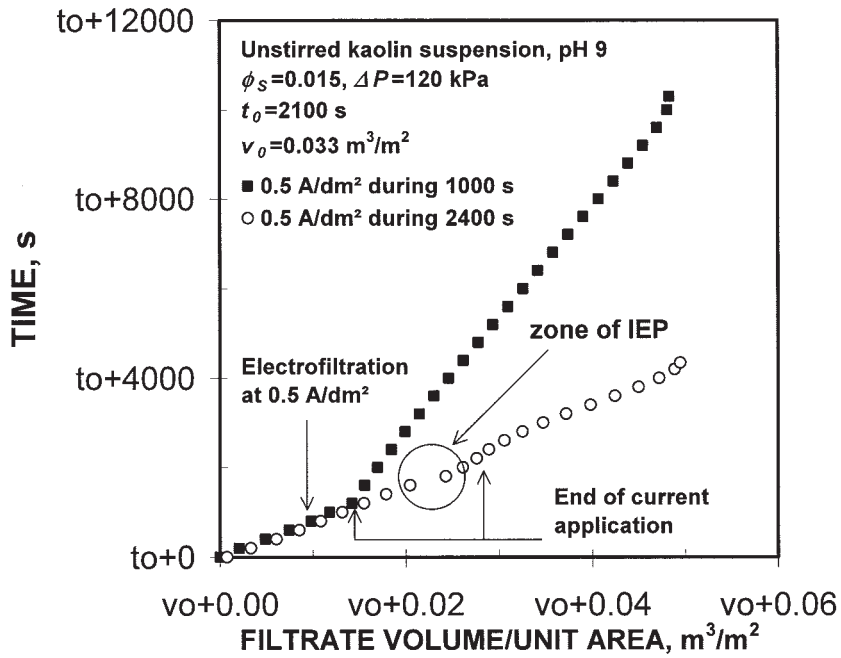

Figure 8. Influence of electrofiltration time on a subsequent filtration under constant pressure.

Table 3. Electrical Parameters, Gas and Heating Production in Electrofiltration

Current (A/dm^2)	Voltage (V)	E (V/m)	$u_E \times 10^{-6}$ (m/s)	ΔT (°C/min)	Gas Volume (μL/min)	Energy (kWh/m^3)
0.2	14.0 ± 1.0	277 ± 6	1.54 ± 0.03	0.04	26	8
0.3	17.8 ± 1.0	350 ± 10	1.97 ± 0.06	0.08	43	14
0.5	28.5 ± 0.8	580 ± 15	3.25 ± 0.08	0.23	69	32
1.0	41.2 ± 2.0	850 ± 40	4.69 ± 0.18	0.92	138	51

produce base and acid at low electrical cost by separating the basic filtrate of the first electrofiltration period and the liquid acid of the subsequent filtration period. Although containing salts, the base and acid produced could be useful in some industrial treatments (such as washing operations).

Applicability of electrofiltration model

The mathematical models of Eqs. 9 and 15 assume that the relative settling velocity and electrophoretic velocity are constant. However, significant changes affecting the particles' ζ-potential throughout the sediments and within the filter cake influenced the electrophoretic velocity and settling velocity. The evaluation of these velocities required an approximation. The rate of solid deposition onto the cake surface may be expressed as $(u_{SR} - u_E)$, where u_{SR} is the relative settling velocity in ordinary filtration at pH 9 ($=6.1 \times 10^{-6}$ m s^{-1}). This approximation is valid during the first period of electrofiltration because the lower part of settling sediments is alkalified and is close to pH 9. The electrophoretic mobility $k \cong 5.6 \times 10^{-9}$ m^2 V^{-1} s^{-1} was determined from Eq. 20 using the value of particle ζ-potential at pH 9. Data from electrofiltrations at various constant current intensities (0.2, 0.3, 0.5, and 1.0 A/dm^2) are shown in Table 3. Table 3 shows, among other parameters, the registered voltage, the electric field intensity (voltage/unit of electrodes spacing), and the electrophoretic velocity as estimated by Eq. 2.

An extended electrofiltration implied heat generation and gas production. Hydrogen produced at the cathode was released in air, whereas oxygen bubbles accumulated over time at the anode side. Table 3 gives the volume of O_2 generated by electrolysis per minute of applied current, calculated by the Faraday's Eq. 17. For instance, the Faraday concentration of O_2 was $n_p = 2 \times 10^{-4}$ mol for 2000 s at 0.5 A/dm^2. The volume of filtrate/unit area displaced by the gas, given by $n_p v_{mol}$, was then 2.7×10^{-3} m^3/m^2. The proportion of the gas was confirmed by visual observation. The filtrate volume was increased by about 13%, attributed to gas production in the electrofiltration period at every current intensity. The gas volume was then taken into account in Eq. 9 using Eq. 18. Table 3 also shows how the temperature and energy consumption (in kWh/m^3 of filtrate) increased during electrofiltration. The temperature increase ΔT was proportional to the squared value of current intensity and thus was significant at the highest current intensity of 1 A/dm^2. The same observation can also be made about energy consumption. The expected decrease in liquid viscosity for an applied current intensity of 0.5 A/dm^2 would be about 10% for 1000 s of electrofiltration ($\Delta T = 4$°C) and 20% for 2000 s of electrofiltration ($\Delta T = 10$°C), based on data given by Cho et al. (1999). Because the theoretical relations are based on a constant viscosity assumption, their applicability seems to be limited to the early electrofiltration period only, specifically when the influence of temperature may be considered negligible. The application of the electrofiltration model is arbitrarily limited to a ΔT of 3°C, which corresponds to an electrofiltration time of 70 min at a current intensity of 0.2 A/dm^2 vs. only 3 min at 1 A/dm^2.

Application of electrofiltration model

In Figure 9, electrofiltration runs at various current intensities, 0.2, 0.3, 0.5, and 1.0 A/dm^2 shown in Table 2, are presented in $(t + t_0)$ vs. $(v + v_0)$ coordinates. The time $t_0 = 2100$ s corresponds to the moment of electric current application after preliminary filtration (Figure 6) and v_0 is the corresponding filtrate volume/unit area. After a 2100-s filtration period, the v_{eq} coefficient in Eq. 9 must take into account the resistance of the cake in addition to that of the filter medium. Therefore, v_{eq} given by Eq. 11 becomes

$$v_{eq} = \frac{R_C + R_m}{\alpha_{av} c_0} \cong \frac{R_C}{\alpha_{av} c_0} \cong \frac{w_{t_0}}{c_0} \tag{24}$$

where w_{t_0} is the mass of dry cake/unit area at the filtration time t_0. The value of v_{eq} for the filtration time $t_0 = 2100$ s was $v_{eq} = 0.0466$ m^3/m^2. The q_{SE} coefficient in Eq. 9, which represents a measure of settling and electrophoretic effects, was approximated by $q_{SE} \cong u_E - u_{SR}$ from Eq. 6. As shown in Figure 9, the electrofiltration model of Eq. 9 with $q_{SE} \cong u_E - u_{SR}$ and $v_{eq} = 0.0466$ m^3/m^2 was satisfactorily fit with experimental data. Electrofiltration runs similar to those presented in Figure 9 were also carried out on stirred suspensions after 4200 s of preliminary filtration. The simplified Eq. 9 using $q_{SE} \cong u_E$ (as $u_{SR} = 0$ in stirred suspension) and $v_{eq} = 0.0466$ m^3/m^2 was also satisfactorily fit with the experimental data. Table 2 indicates the correlated K_E coefficients for electrofiltration with sedimentation (EF + S) and electrofiltration with agitation (EF) at several electric field magnitudes. It is worth noting that the K_E coefficient, which is a measure of the electroosmotic effect, can be expressed in terms of an empirical relationship as follows (Iritani et al., 1992)

$$K_E = K_{E0} + aE \qquad \text{where } a = 1.4 \times 10^{-9} \text{ m}^3 \text{ V}^{-1} \text{ s}^{-1} \tag{25}$$

This result implies that the electroosmotic effect in electrofiltration becomes more marked as E increases. The unknown electroosmotic pressure in Eq. 9 was deduced from the correlated K_E coefficient by means of Eq. 10 using $\mu = 0.001$ Pa·s, $\Delta P = 120$ kPa, $c_0 = 38.5$ kg/m^3, and the average specific cake resistance obtained in filtration with sedimentation, $\alpha_{av} = 9.1 \times 10^{12}$ m/kg. The electroosmotic pressure can be extracted from the electroosmotic flow q_E during the constant rate period (EP) by means of Eq. 15. Also, it can be obtained from fitting

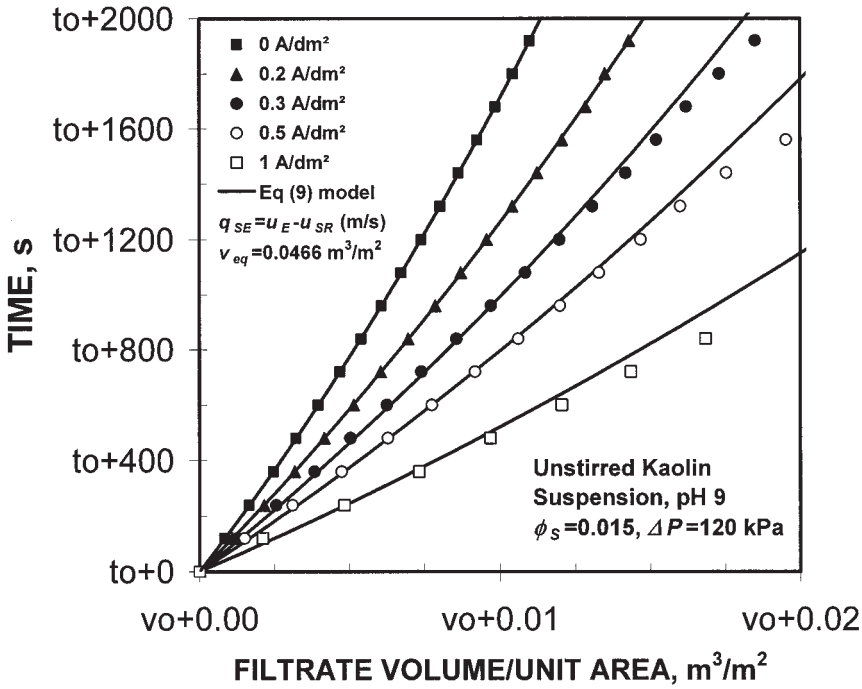

Figure 9. Data fit of the electrofiltration predictive model with data from sedimentation tests under constant pressure at various electric field magnitudes.

the models to data from the (EF) and (EF + S) processes (Eq. 9). The values of ΔP_E calculated for different electrofiltration processes were close, as shown in Table 2. Therefore, the developed electrofiltration model seems to represent well the experimental data from kaolin suspensions.

Influence of particle settling

For the studied kaolin suspension, the influence of settling on electrofiltration rate remained rather low compared to electrokinetic effects that contribute by approximately 55% to the decrease of filtration time for the same filtrate volume at a current intensity of 0.5 A/dm^2. In Figure 10, the electrofiltration model is presented in $(t + t_0)$ vs. $(v + v_0)$ coordinates at various current intensities: 0, 0.5, and 1.0 A/dm^2, v_{eq} is taken as $v_{eq} = 0.0466$ and the average value of K_E is as mentioned in Table 2. For every current intensity, both q_{SE} coefficients were considered: $q_{SE} \cong u_E - u_{SR}$ (presence of sedimentation) and $q_{SE} \cong u_E$ (absence of sedimentation). In the particular case of $q_{SE} = 0$ (filtration without sedimentation), Ruth's Eq. 13 was used instead of Eq. 9. The settling effect enhances the cake formation and therefore the resistance to liquid flow and compensates for the electrokinetic effects. For the studied kaolin suspension with $u_{SR} = 6.1 \times 10^{-6}$ m/s, the settling effect is not very significant. However, it may be speculated that higher settling velocity would have a major impact on electrofiltration. Figure 11 presents the influence of settling velocities on electrofiltration, based on the proposed model, and using the K_E and v_{eq} coefficients obtained at 0.5 A/dm^2. Curve 1 represents electrofiltration without sedimentation ($q_{SE} \cong u_E$) and curve 2 shows electrofiltration with the real relative settling velocity obtained experimentally ($q_{SE} \cong u_E - u_{SR}$). Extrapolations are made in Figure 11 using Eq. 9 with simulated higher settling velocities ($2u_{SR}$ and $4u_{SR}$). High settling velocities should have considerable impact on electrofiltration, as shown in Figure 11 in curves 3 and 4 ($q_{SE} \cong u_E - 2u_{SR}$ and $q_{SE} \cong u_E - 4u_{SR}$). A relative sedimentation velocity of $4u_{SR} - u_E = 2.1 \times 10^{-5}$ m/s (curve 4), would cause a 25% reduction in filtrate volume (at $t = 1800$ s) compared to the electrofiltration shown in curve 1 that involves only electrokinetic effects.

Conclusion

This article has reported the experimental and theoretical study of batch electrofiltration, accompanied by side effects of particle sedimentation and water electrolysis involving production of gas, hydroxide, and hydronium ions. The electrofiltration process was applied to a kaolin suspension at pH 9 using various electric field magnitudes. Side effects showed considerable positive impact on the electrofiltration behavior. Electrolytic gas accumulated in upper anode side and displaced the suspension in the downward direction, increasing by 13% the downward electrofiltration rate. Electrolysis ionic products generated a distribution of pH inside the filter that became gradually alkalified at the cathode and acidified in the filtered suspension. During electrofiltration, a decrease in pH was observed near the anode, leading to particle coagulation, and the decrease in pH propagated throughout the filter cake led to a coagulation of cake particles. This coagulation effect is associated with a significant decrease of the specific cake resistance that subsequently allowed an ordinary filtration at a velocity comparable to that obtained in electrofiltration. Electrofiltration significantly reduced the process cycle time (half the time of ordinary filtration), which indicates the importance of this process for industrial applications. Furthermore, electrofiltration was applied only during 37% of process cycle time (preliminary filtration = 2100 s, electrofiltration $\cong$ 2400 s, subsequent ordinary filtration $\cong$ 1900 s). Just like kaolin, many

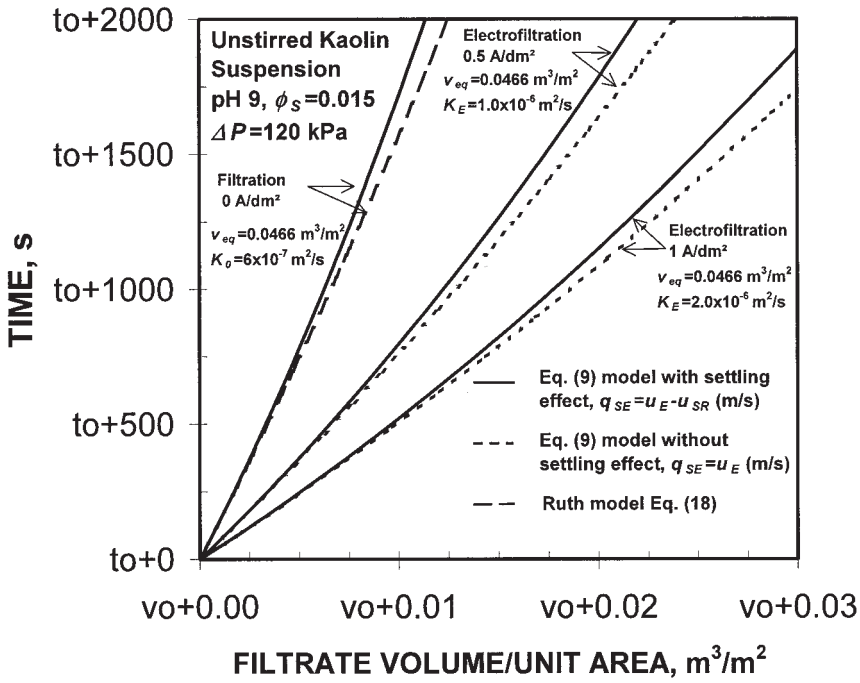

Figure 10. Effect of settling on electrofiltration behavior as predicted by the electrofiltration model with or without settling effect.

mineral or biological particles are highly dependent on pH and should be amenable to coagulation using electrofiltration. This coagulation effect may then provide a useful means of accelerating filtration kinetics, without proceeding to a full-time electrofiltration, and thus achieving considerable energy savings.

As in ordinary filtration, the sedimentation of the particles leads to an underestimation of the amount of particles deposited onto the filter cake. Therefore, the settling effect in electrofiltration should not be neglected, especially in suspensions where the settling velocity is significant. The mathematical model developed to take into account the production of electrolytic gas and the sedimentation of particles accounted well for experimental data in the early stages of electrofiltration. As

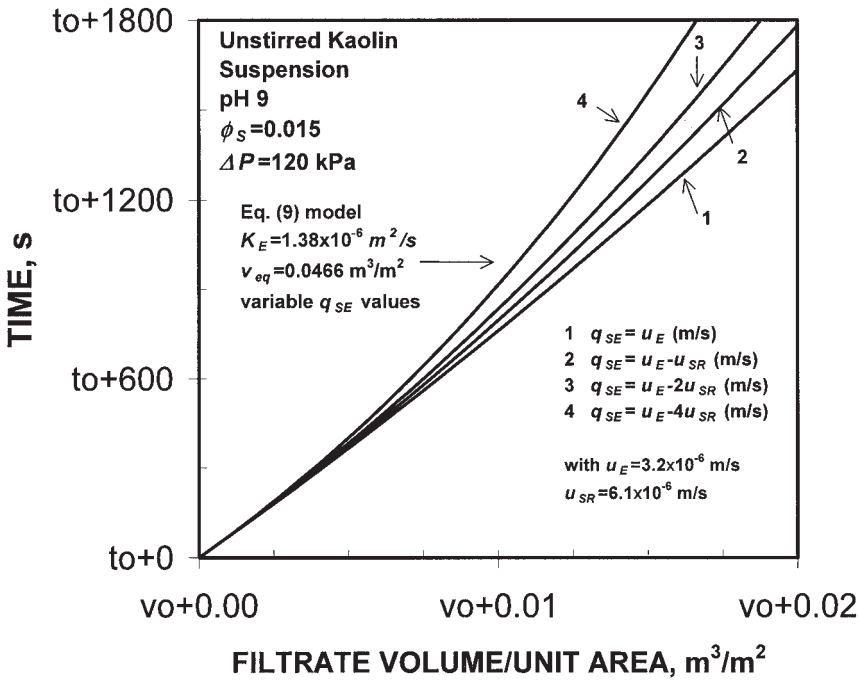

Figure 11. Representation of predictive electrofiltration model with an increasing settling velocity of sediments.

the electrofiltration process progressed, the model is no longer valid because of a decrease in viscosity under thermal effects and the alteration of cake permeability by ionic electrolytic products. Finally, future optimization of the electrofiltration process will require taking into account various side effects.

Notation

K_E = coefficient in Eq. 9, m^2/s
K = coefficient in Eq. 13, m^2/s
q = filtrate flow rate, m/s
q_{SE} = coefficient in Eq. 9, m/s
q_S = coefficient in Eq. 9 in the absence of electric field, m/s
q_E = coefficient in Eq. 9 in the absence of particles settling, m/s
q_E = coefficient in Eqs. 14 and 15, m/s
T = temperature inside the filter cake, °C
v = filtrate volume/unit filter area, m^3/m^2
v_{eq} = coefficient in Eqs. 9 and 13, m^3/m^2
ϕ_S = volume fraction of solid in liquid
μ = filtrate viscosity, Pa·s
ρ_l = density of the liquid, kg/m^3
ρ_S = density of the solid particles, kg/m^3

Literature Cited

Barton, W. A., S. A. Miller, and C. J. Veal, "The Electrodewatering of Sewage Sludges," *Drying Technol.*, **17**, 497 (1999).

Bazhal, M., and E. Vorobiev, "Electrical Treatment of Apple Cossettes for Intensifying Juice Pressing," *J. Sci. Food Agric.*, **80**, 1668 (2000).

Biesheuvel, P. M., and H. Verweij, "Influence of Suspension Concentration on Cast Formation Time in Pressure Filtration," *J. Eur. Ceram. Soc.*, **20**, 835 (2000).

Bockstal, F., L. Fouarge, J. Hermia, and G. Rahier, "Constant Pressure Cake Filtration with Simultaneous Sedimentation," *Filtr. Sep.*, **22**, 255 (1985).

Cho, C. H., J. Urquidi, and G. W. Robinson, "Molecular-Level Description of Temperature and Pressure Effects on the Viscosity of Water," *J. Chem. Phys.*, **111**, 10171 (1999).

Iritani, E., Y. Mukai, and H. Yorita, "Effect of Sedimentation on Properties of Upward and Downward Cake Filtration," *Kagaku Kobaku Ronbunshu*, **25**, 742 (1999).

Iritani, E., K. Ohashi, and T. Murase, "Analysis of Filtration Mechanism of Dead-End Electro-Ultrafiltration for Proteinaceous Solutions," *J. Chem. Eng. Jpn.*, **25**, 383 (1992).

Iwata, M., H. Igami, and T. Murase, Analysis of Electroosmotic Dewatering, *J. Chem. Eng. Jpn.*, **24**, 45 (1991).

Jujikov, V., *Filtration*. Chemistry, Moscow (1971).

Kondo, S., and M. Hiraoka, "Commercialization of Pressurized Electroosmotic Dehydrator (PED)," *Water Sci. Technol.*, **22**, 259 (1990).

Kynch, G. J., "A Theory of Sedimentation," *Trans. Faraday Soc.*, **48**, 166 (1952).

Larue, O., E. Vorobiev, C. Vu, and B. Durand, "Electrocoagulation and Coagulation by Iron of Latex Particles in Aqueous Suspensions," *Sep. Pur. Technol.*, **31**, 177 (2003).

Lyklema, J., "Electrokinetics after Smoluchowski," *Colloids Surf. A: Physicochem. Eng. Aspects*, **222**, 5 (2003).

Moulik, S. P., "Physical Aspects of Electrofiltration," *Curr. Res.*, **5**, 771 (1971).

Orsat, V., G. S. V. Raghavan, S. Sotocinal, D. G. Lightfoot, and S. Gapolakrishnan, "Roller Press for Electroosmotic Dewatering of Biomaterials," *Drying Technol*., **17**, 523 (1999).

Raats, M. H. M., A. J. G. Van Diemen, J. Laven, and H. Stein, "Full Scale Electrokinetic Dewatering of Waste Sludge," *Colloids Surf. A: Physicochem. Eng. Aspects*, **210**, 231 (2002).

Ruth, B. F., "Correlating Filtration Theory with Industrial Practice," *Ind. Eng. Chem.*, **38**, 564 (1946).

Tarleton, E. S., R. J. Wakeman, and Y. Liang, "Electrically Enhanced Washing of Ionic Species from Fine Particle Filter Cakes," *Trans. IChemE*, **81**, 201 (2003).

Tiller, F. M., N. B. Hsyung, and D. Z. Cong, "Role of Porosity in Filtration: XII. Filtration with Sedimentation," *AIChE J.*, **41**, 1153 (1995).

Vorobiev, E., and S. Jany, "Etapes de filtration frontale assistée par un champ électrique," *Entropie*, **219**, 23 (1999).

Wakeman, R. J., "The Formation and Properties of Apparently Incompressible Filter Cakes under Vacuum on Downward Facing Surfaces," *Trans. IChemE*, **59**, 260 (1981).

Wakeman, R. J., and E. S. Tarleton, *Filtration: Equipment Selection, Modelling and Process Simulation*, Elsevier, Oxford, UK (1998).

Weber, K., and W. Stahl, "Improvement of Filtration Kinetics by Pressure Electrofiltration," *Sep. Pur. Technol.*, **26**, 69 (2002).

Yoshida, H., K. Kitajyo, and M. Nakayama, "Electroosmotic Dewatering under A.C. Electric Field with Periodic Reversals of Electrode Polarity," *Drying Technol.*, **17**, 539 (1999).

Yukawa, H., H. Chigira, T. Hoshino, and M. Iwata, "Fundamental Study of Electroosmotic Filtration," *J. Chem. Eng. Jpn.*, **4**, 370 (1971).

Yukawa, H., K. Kobayashi, Y. Tsukui, S. Yamano, and M. Iwata, "Analysis of Batch Electrokinetic Filtration," *J. Chem. Eng. Jpn.*, **9**, 396 (1976).

Manuscript received Aug. 20, 2003, and revision received Mar. 26, 2004.